Egyptian Journal of Petroleum (2015) 24, 493–503

HOSTED BY

ELSEVIER

Egyptian Petroleum Research Institute

Egyptian Journal of Petroleum

www.elsevier.com/locate/egyjp
www.sciencedirect.com

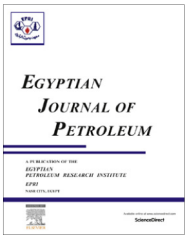

FULL LENGTH ARTICLE

The performance of hydrophobic and hydrophilic moieties in synthesized thiol cationic surfactants on corrosion inhibition of carbon steel in HCl

E.M.S. Azzam [a,*], M.A. Hegazy [a], N.G. Kandil [b], A.M. Badawi [a], R.M. Sami [a]

[a] *Egyptian Petroleum Research Institute (EPRI), Nasr City, Cairo, Egypt*
[b] *Faculty of Women–Ain Shams University, Cairo, Egypt*

Received 12 October 2014; revised 15 February 2015; accepted 18 February 2015
Available online 4 November 2015

KEYWORDS

Thiol surfactants;
Hydrophilic and hydrophobic moieties;
Carbon steel;
Acid medium

Abstract Here in, cationic surfactants namely (1-octyl, decyl, and dodecyl-4-mercaptopyridine-1-ium bromide) I, II and III, respectively, were synthesized. The inhibition effect of these surfactants on the corrosion of carbon steel in 1 M HCl was studied by polarization, electrochemical impedance spectroscopy (EIS) and weight loss measurements. Polarization curves revealed that the used inhibitors represent mixed-type inhibitors. Adsorption of used inhibitors led to a reduction in the double layer capacitance and an increase in the charge transfer resistance. Adsorption of used compounds was found to obey Langmuir isotherm.

1. Introduction

The carbon steel is used as essential part in the manufacturing of installations used in the petroleum and other industries [1–4]. Acid solutions are widely used in industry, chemical cleaning, descaling and pickling, which lead to corrosive attack. The majority of the well-known inhibitors are organic compounds containing heteroatoms, such as oxygen, nitrogen or sulfur and multiple bonds, which allow an adsorption on the metal surface. It has been observed that the adsorption of these inhibitors depends on the physicochemical properties of the functional groups and the electron density at the donor atom. The adsorption occurs due to the interaction of the lone pair and/or p-orbitals of inhibitor with d-orbitals of the metal surface atoms, leading to the formation of a corrosion protection film [5,6]. Adsorption is also influenced by the structure and the charge of metal surface, and the type of testing electrolyte [7]. A large number of organic compounds were studied as corrosion inhibitors for iron and low carbon steels [8].

Fortunately, many researchers have explored this field, and many useful analytical methodologies have been developed [9,10]. Since corrosion inhibition depends on the ability of a surfactant inhibitor to adsorb, which is directly related to its capacity to aggregate to form micelles. The critical micelle concentration (C_{cmc}) is a key indicator in determining the corrosion inhibition effectiveness of the surfactant concentration increase. The individual surfactant ions or monomer tends to migrate to the interface which reduces surface tension, and if it occurs on metal surface, it will inhibit corrosion. Above

* Corresponding author. Tel.: +20 1117710207; fax: +20 222747433.
E-mail address: eazzamep@yahoo.com (E.M.S. Azzam).

Peer review under responsibility of Egyptian Petroleum Research Institute.

http://dx.doi.org/10.1016/j.ejpe.2015.02.012

the C_{cmc}, the surface is covered with a mono layer, thus any additional surfactant molecules that are added to the solution above the C_{cmc} level will combine to form micelles or multiple layers of adsorbed surfactant molecules or form micelles in the bulk of corrosive medium. As a result, the surface tension and corrosion current density are not altered significantly above the C_{cmc}. Consequently, an excellent surfactant inhibitor is one with a low C_{cmc} value, whereas, a surfactant with a high C_{cmc} value, will be a less effective inhibitor at the same concentration.

The purpose of this work is to investigate the performance of the alkyl chain length and thiol group in the synthesized cationic surfactants on corrosion inhibition efficiency of carbon steel in 1 M HCl using weight loss, potentiodynamic polarization and electrochemical impedance spectroscopy techniques. The thermodynamic parameters of inhibitor adsorption on the metal surface and metal dissolution were also studied. Surface properties of the synthesized surfactant in bulk solution such as the critical micelle concentration (C_{cmc}), effectiveness of surface tension reduction (π_{cmc}), surface excess concentration (Γ_{max}) and surface area per molecule (A_{min}) were determined by means of surface tension measurements. In addition, the free energies of micellization (ΔG^{o}_{mic}) and adsorption (ΔG^{o}_{ads}) were calculated. Moreover, the behavior and the relation between molecular structure, surface properties, and the inhibitive effects of these compounds on corrosion inhibition of carbon steel in 1 M HCl solution were investigated and discussed.

2. Materials and experimental techniques

2.1. Synthesis of the thiol cationic surfactants

The cationic thiol surfactants were synthesized by a reaction of alkyl halides with different alkyl chain lengths (octyl-, decyl- and dodecyl-bromide) with appropriate amount of 4-mercapto pyridine in the molar ratio of 1:1 to produce 1-octyl, decyl, and dodecyl-4-mercapto pyridine-1-ium bromide, as shown in Fig. 1. The reactants were allowed to reflux in ethanol for 50 h. Then the reaction mixture was left to cool to room temperature. The product was purified and recrystallized from diethylether and ethanol, respectively, then filtrated and dried to obtain the synthesized cationic surfactants.

2.2. Solutions

Aggressive solutions (1 M HCl) were prepared by dilution of analytical grade 37% HCl with distilled water. The concentrations of the prepared cationic surfactants ranged from 5×10^{-4} to 10^{-2} M for corrosion measurements and from 10^{-4} to 10^{-2} M for surface tension and conductivity. All solutions were prepared using distilled water.

2.3. Weight loss measurements

The carbon steel sheets of 2.5 cm × 7.5 cm × 0.5 cm were abraded with a series of emery paper (grade 320–500–800–1000–1200) and then washed with distilled water and acetone. After weighing accurately, the specimens were immersed in 150 ml closed beaker, which contained 100 ml 1 M HCl with and without addition of different concentrations of inhibitors. After 24 h, the specimens were taken out, washed, dried and weighed accurately. Experiments were carried out in triplicate. The average weight loss of three parallel carbon steel sheets was obtained. Chemical composition of carbon steel sample is listed in Table 1.

2.4. Electrochemical measurements

Electrochemical experiments were carried out using a Voltalab 40 Potentiostat PGZ 301 in a conventional electrolytic cell with three-electrode arrangement: saturated calomel reference electrode (SCE), platinum rod as a counter electrode and the working electrode (WE) had the form of a rod from carbon

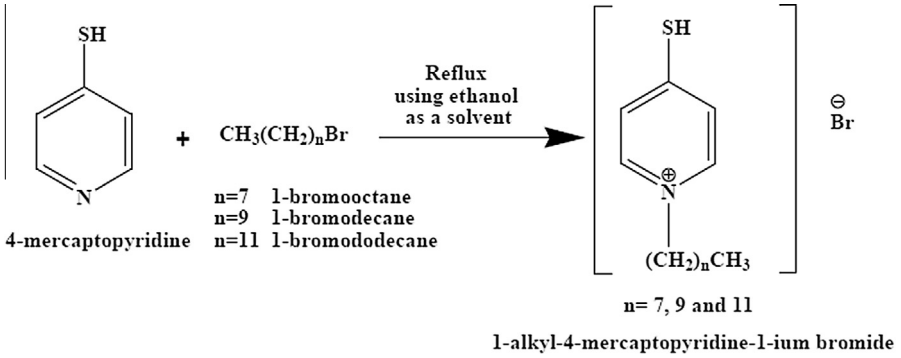

Figure 1 The chemical reaction of the prepared cationic surfactants.

Table 1 Chemical composition of carbon steel sample.

Element	C	Si	Mn	P	S	Ni	Cr	Al	V	Ti	Cu	Fe
Weight %	0.19	0.05	0.94	0.009	0.004	0.014	0.009	0.034	0.016	0.003	0.022	Reminder

steel. Prior to each experiment, the specimen was treated as in weight loss measurements.

The electrode potential was allowed to reach equilibrium 30 min before starting the measurements. The exposed electrode area to the corrosive solution is 0.7 cm^2. All experiments were conducted at 25 °C. Potentiodynamic polarization curves were obtained by changing the electrode potential automatically (from −800 to −300 mV vs. SCE) at open circuit potential with a scan rate of 2 mV s^{-1}.

EIS measurements were carried out in a frequency range of 100 kHz to 50 mHz with amplitude of 4 mV peak-to-peak using ac signals at open circuit potential. All experiments' data were analyzed by VoltaMaster 4 program which is combined with VoltaLab device.

2.5. Surface tension measurements

Surface tension was measured with a Du Nouy Tensiometer (Kruss Type 6) for different concentrations of synthesized cationic surfactants. Doubly distilled water from an all-glass apparatus with a surface tension of 72 mN m^{-1} at 25 °C was used to prepare all solutions.

2.6. Conductivity measurements

Specific conductivity was measured with a digital conductivity meter (Type 522; Crison Instrument, S.A.) using a double jacket glass cell. The cell constants were determined using KCl solutions. All measurements were done in a jacketed vessel at 25 °C, which was maintained at the appropriate temperature (±0.5 °C).

3. Results and discussion

3.1. Chemical structure confirmation of the synthesized cationic surfactants

The chemical structures of the prepared cationic surfactants were confirmed by the FTIR and ^{1}H NMR spectroscopy and are shown in Figs. 2 and 3.

3.1.1. FTIR spectra

The FTIR spectra in Fig. 2 of the synthesized surfactants I, II and III showed the following absorption band peaks at 2581 cm^{-1} (sym CH_2), 2920 cm^{-1} (asym CH_2), 2604 cm^{-1} (sym SH) very weak band, 1590 cm^{-1} (C═C Ar), 1473 cm^{-1} (CH_2 binding), 1623 cm^{-1} (C═N), 1195 cm^{-1} (C–N) and sym (C–S) bands around 620 cm^{-1}. The shift and the intensity of the peaks depend on the difference in the alkyl chain length of surfactants.

3.1.2. ^{1}H NMR spectra

The ^{1}H NMR spectra of inhibitor III showed different bands at δ = 0.7983–0.825 ppm (t, 3H, CH_3) , δ = 1.1988–1.3.837 ppm (m, 16H, CH_2), δ = 1.6175–1.6481 ppm (q, 2H, beta CH_2), δ = 3.4517 ppm (s, 1H, SH), δ = 3.1934–3.2239 ppm (t, 2H, N-CH_2), δ = 7.8292 ppm (d, 2H, pyridine), δ = 7.8429 ppm (d, 2H, pyridine), δ = 8.5689 (d, 2H, pyridine), δ = 8.5827 (d, 2H, pyridine).

3.2. Weight loss measurements

The corrosion rate (k) was calculated from the following equation [11]:

$$k = \frac{W}{St} \tag{1}$$

where W is the average weight loss of three parallel carbon steel sheets, S is the total area of the specimen and t is the immersion time.

The inhibition efficiency (η_w) and surface coverage (θ) of inhibitor on the surface of carbon steel were calculated using the following equations:

$$\eta_w = \left(\frac{k^o - k}{k^o}\right) \times 100 \tag{2}$$

$$\theta = \frac{k^o - k}{k^o} \tag{3}$$

where, k^o and k are the values of the corrosion rate without and with addition of the inhibitor, respectively.

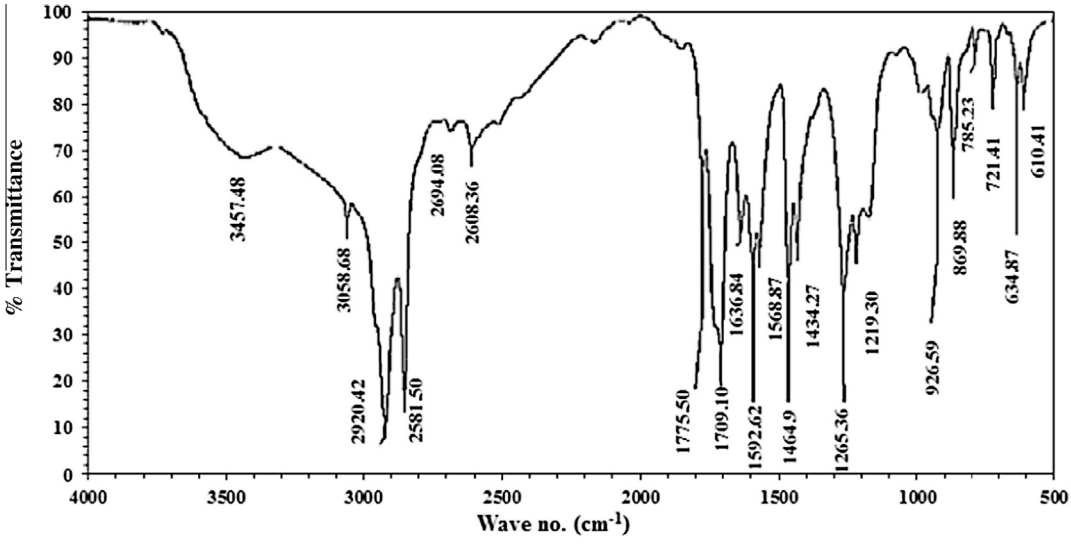

Figure 2 FTIR spectrum of 4-mercapto-N-decylpyridinium bromide III.

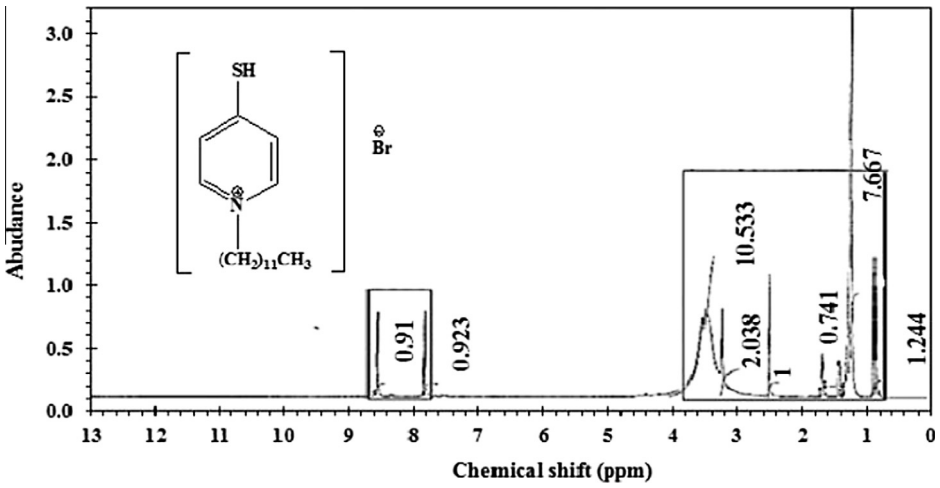

Figure 3 ^{1}H NMR spectrum of 4-mercapto-N-decylpyridinium bromide III.

The corrosion parameters such as corrosion rate k, inhibition efficiency η_w and surface coverage θ at different concentrations of the synthesized surfactants in 1 M HCl at 25 °C, 40 °C and 60 °C are listed in Table 2. It was found that the synthesized surfactants inhibit the corrosion of carbon steel at all concentrations in 1 M HCl. These data showed that the corrosion rate values decreased as the concentrations of the inhibitor increased, i.e. the corrosion inhibition efficiency increased with increasing the inhibitor concentration. This behavior was due to the adsorption and the coverage of inhibitors on carbon steel surface. Also, the data in Table 2 showed that the corrosion rate of steel increased with increasing temperature for both uninhibited and inhibited solution. The corrosion rate of steel increased more rapidly with temperature increasing in the absence of the inhibitor molecules. These results confirmed that the synthesized inhibitors acted as an efficient inhibitor in the range of the temperatures studied.

The maximum corrosion inhibition efficiency for all compounds was obtained at 10^{-2} M. The corrosion inhibition efficiency of the investigated inhibitors decreased in the following order

III > II > I

Fig. 4 shows the relation between η_w of carbon steel and logarithm of the concentration of the prepared inhibitors.

Table 2 Weight loss results of carbon steel corrosion with and without different concentrations of the synthesized cationic surfactants at 25 °C in 1 M HCl.

Inhibitor	Inhibitor conc. (M)	25 °C			40 °C			60 °C		
		k mg cm^{-2} h^{-1}	θ	η_w %	k mg cm^{-2} h^{-1}	θ	η_w %	k mg cm^{-2} h^{-1}	θ	η_w %
Absence	1.0 M HCl	1.137			2.020			4.03		
I	5.0×10^{-4}	0.3961	0.65	65.17	0.7750	0.62	61.63	1.7763	0.56	55.92
	1.0×10^{-3}	0.2948	0.74	74.08	0.6369	0.68	68.47	1.5222	0.62	62.22
	2.5×10^{-3}	0.2158	0.81	81.03	0.5409	0.73	73.22	1.2193	0.70	69.74
	5.0×10^{-3}	0.1793	0.84	84.23	0.4102	0.80	79.69	1.1147	0.72	72.34
	7.5×10^{-3}	0.1155	0.90	89.84	0.3192	0.84	84.19	0.8437	0.79	79.06
	1.0×10^{-2}	0.0866	0.92	92.39	0.2266	0.89	88.78	0.6592	0.84	83.64
II	5.0×10^{-4}	0.298	0.74	73.84	0.746	0.63	63.07	1.735	0.57	56.93
	1.0×10^{-3}	0.203	0.82	82.16	0.592	0.71	70.70	1.363	0.66	66.18
	2.5×10^{-3}	0.151	0.87	86.76	0.504	0.75	75.06	1.146	0.72	71.56
	5.0×10^{-3}	0.106	0.91	90.65	0.371	0.82	81.64	1.005	0.75	75.05
	7.5×10^{-3}	0.076	0.93	93.30	0.270	0.87	86.63	0.766	0.81	81.00
	1.0×10^{-2}	0.054	0.95	95.27	0.191	0.91	90.53	0.577	0.86	85.68
III	5.0×10^{-4}	0.218	0.81	80.83	0.689	0.66	65.87	1.507	0.63	62.60
	1.0×10^{-3}	0.142	0.87	87.49	0.556	0.72	72.45	1.281	0.68	68.22
	2.5×10^{-3}	0.110	0.90	90.29	0.484	0.76	76.06	1.066	0.74	73.55
	5.0×10^{-3}	0.087	0.92	92.36	0.361	0.82	82.10	0.963	0.76	76.09
	7.5×10^{-3}	0.061	0.95	94.66	0.233	0.88	88.45	0.709	0.82	82.40
	1.0×10^{-2}	0.044	0.96	96.09	0.167	0.92	91.71	0.508	0.87	87.38

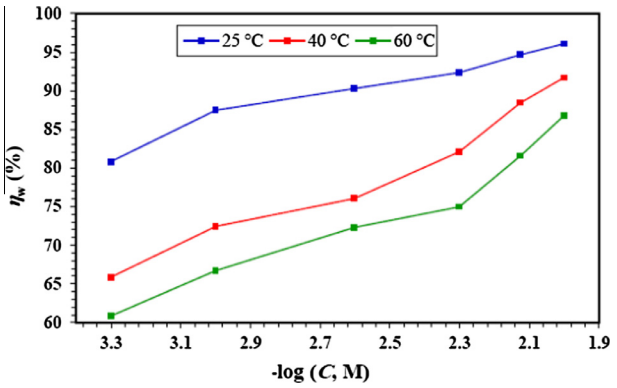

Figure 4 The relation between corrosion inhibition efficiency of carbon steel and logarithm of the concentration of the prepared inhibitors.

3.3. Polarization measurements

Fig. 5 shows the polarization curves of carbon steel in 1 M HCl in the absence and presence of different concentrations of corrosion inhibitors III. On inspection of Fig. 5, it is observed that the current density of the anodic and cathodic branches is displaced toward lower values. This displacement is more evident with the increase in concentration of the corrosion inhibitor when compared to the blank. The electrochemical parameters, such as corrosion current density (i_{corr}), anodic (β_a) and cathodic (β_c) slopes, were obtained by Tafel extrapolation at the corrosion potential (E_{corr}) and are reported in Table 3. It is observed that the corrosion current density decreased when the inhibitor concentration increased and the lowest values were obtained for III at 10^{-2} M. The

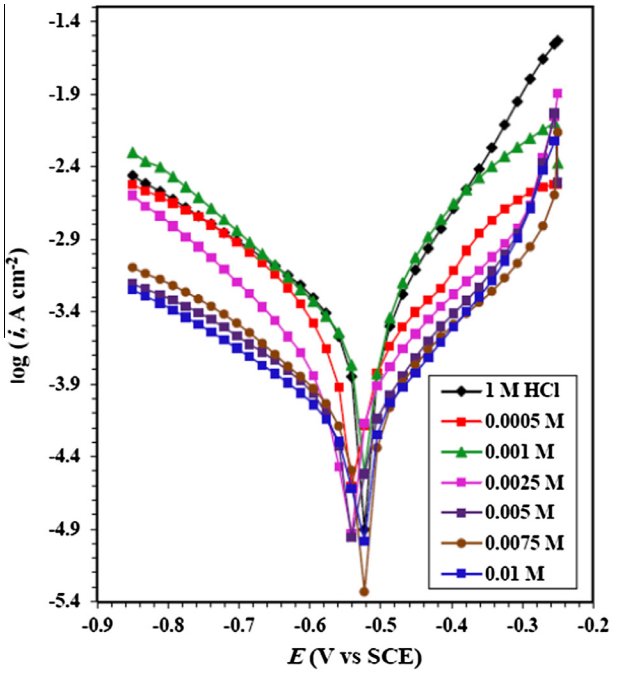

Figure 5 Anodic and cathodic polarization curves obtained at 25 °C in 1 M HCl in different concentrations of III.

anodic and cathodic slopes do not display an order with the inhibitor concentration; this feature indicates that corrosion inhibitors have no effect on both hydrogen evolution and iron dissolution mechanism, it appears that inhibition occurred by a blocking mechanism on the available metal spaces [12]. These results indicated that the presence of cationic surfactants as inhibitors inhibited iron oxidation and to a lower extent the hydrogen evolution, consequently these compounds can be classified as mixed corrosion inhibitors [13]. The inhibition efficiency (η_p) was calculated from the polarization curves as follows:

$$\eta_p = \left(\frac{i^o_{corr} - i_{corr}}{i^o_{corr}}\right) \times 100 \quad (4)$$

where i^o_{corr} and i_{corr} are uninhibited and inhibited current densities, respectively.

The potential E_{corr} values in the presence of different concentrations of the synthesized inhibitors are slightly shifted toward both positive and negative directions compared to blank, suggesting that the inhibitor is a mixed type inhibitor (that is, inhibit both anodic and cathodic reactions) and is adsorbed on the surface there by blocking the corrosion reaction centers. The best inhibition efficiency was III of about 95.50 % at 10^{-2} M.

3.4. Electrochemical impedance measurements

Fig. 6 shows Nyquist plots for carbon steel in 1 M HCl solutions with and without various concentrations of inhibitor III as representative from the tested inhibitors at 25 °C. It can be observed that the impedance response behavior of carbon steel shows a significant change after the addition of the inhibitors in 1 M HCl solution. Comparing between the semicircle radii of the carbon steel in uninhibited solution and these in presence of the different inhibitors showed that the real axis intercept at low frequencies in the presence of inhibitor is larger than that in the absence of inhibitor (blank) and increases as the inhibitor concentration increases. This confirms that the impedance of carbon steel corrosion increased with the increase in the inhibitors concentrations in 1 M HCl solution. The impedance of carbon steel corrosion increases due to the increase in the surface coverage of inhibitor molecules on the electrode surface, which results in an increase in the inhibition efficiency. Adsorbed inhibitor molecules form a protective film which insulates the carbon steel surfaces and inhibits both cathodic and anodic reactions of steel surface [14].

It is clear from Fig. 6 that the impedance spectra exhibit one single capacitive loop, which indicates that the formed charge transfer complexes between the metal surface and the inhibitor molecules take place at the electrode/solution interface, and the transfer process controls corrosion reaction. The similar behaviors of the different capacitive loops indicate that the presence of inhibitors does not change the mechanism of carbon steel dissolution. Noticeably, the imperfect semicircles represented in Fig. 6 are related to the frequency dispersion due to the roughness and inhomogeneous of the electrode surface. The EIS results were simulated by the equivalent circuit shown in Fig. 7 to pure electric models that could verify the mechanistic models and enable the calculation of numerical values corresponding to the physical and/or chemical properties of the tested electrochemical system [15]. The cir-

Table 3 Shows the electrochemical corrosion kinetic parameters of carbon steel corrosion with and without different concentrations of the synthesized cationic surfactants at 25 °C in 1 M HCl.

Inhibitor	Conc. of inhibitor (M)	E_{corr} mV (SCE)	i_{corr} mA cm^{-2}	β_a mV dec^{-1}	β_c mV dec^{-1}	θ	η_p %
1 M HCl	0.0	−533.5	1.70	306.1	−252.8	0.00	0.00
I	5.0×10^{-4}	−501.1	0.5572	214	−254.3	0.67	67.13
	1.0×10^{-3}	−510.6	0.4408	193.7	−207.4	0.74	73.99
	2.5×10^{-3}	−525.6	0.34	262.5	−194.5	0.80	80.02
	5.0×10^{-3}	−525.1	0.22	271.7	−279.8	0.87	87.10
	7.5×10^{-3}	525.5	0.18	220	−158.7	0.90	89.52
	1.0×10^{-2}	−5260	0.14	280.9	−506.8	0.92	91.75
II	5.0×10^{-4}	−529.8	0.5434	224.8	−221.4	0.68	67.94
	1.0×10^{-3}	−509.7	0.32	229.4	−267.1	0.81	81.33
	2.5×10^{-3}	−538.3	0.24	293.8	−185.3	0.86	86.01
	5.0×10^{-3}	−536.5	0.16	202.7	−217	0.90	90.47
	7.5×10^{-3}	−546.2	0.14	240.6	−233.1	0.92	91.95
	1.0×10^{-2}	−515	0.09	221.3	−205.4	0.95	94.89
III	5.0×10^{-4}	−541.5	0.3342	275.3	−300.5	0.80	80.28
	1.0×10^{-3}	−525	0.23	112.1	−229.9	0.87	86.51
	2.5×10^{-3}	−534.4	0.14	231.7	−196.5	0.92	91.96
	5.0×10^{-3}	−543.5	0.09	221.3	−205.4	0.95	94.89
	7.5×10^{-3}	−520.6	0.07	218.6	−249.3	0.96	95.89
	1.0×10^{-2}	−524.2	0.06	165.4	−286	0.96	96.44

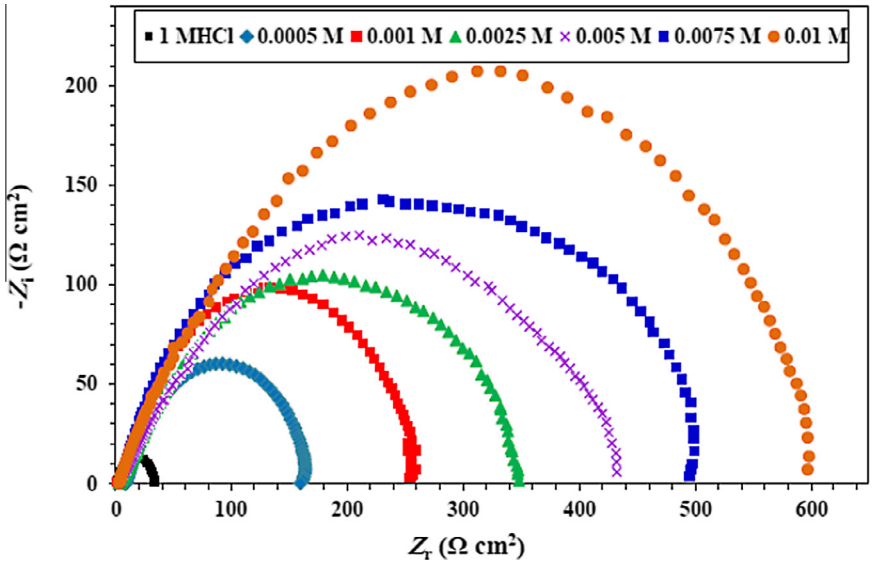

Figure 6 Nyquist plots for carbon steel in 1 M HCl in absence and presence of different concentrations of III.

cuit allows identifying both solution resistances (R_S), charge transfer resistance (R_{ct}) and double layer capacitance (C_{dl}). It is worth mentioning that C_{dl} value is affected by imperfections of the surface, and this effect is simulated by a constant phase element (CPE). The CPE is composed of a component Q_{dl} and a coefficient (n) which quantifies different physical phenomena like surface roughness, inhibitor adsorption, porous layer formation, etc. The C_{dl} can be calculated using Eq. (5) [16]:

$$C_{dl} = Q_{dl} \times (2\pi f_{max})^{n-1} \quad (5)$$

where f_{max} represents the frequency at which imaginary value reaches a maximum on the Nyquist plot.

The inhibition efficiency of the different inhibitors were calculated using Eq. (6):

$$\eta_I = \left(\frac{R_{ct}(\text{uninh}) - R_{ct}(\text{inh})}{R_{ct}(\text{uninh})} \right) \times 100 \quad (6)$$

where, R_{ct}(inh) and R_{ct}(uninh) are the charge-transfer resistances in the inhibited and the uninhibited solutions. The electrochemical parameters of R_{ct}, C_{dl} And η_I listed in Table 4.

Table 4 disclosed that by increasing the inhibitor concentrations R_{ct} values increased significantly and also C_{dl} values decreased. The decrease in C_{dl} values in presence of the different inhibitors compared to the uninhibited solution is due to the decrease in local dielectric constant and/or an increase in the thickness of the electrical double layer, which suggests the adsorption of inhibitor molecules at the metal/solution interface [17]. Increasing the concentration of the added

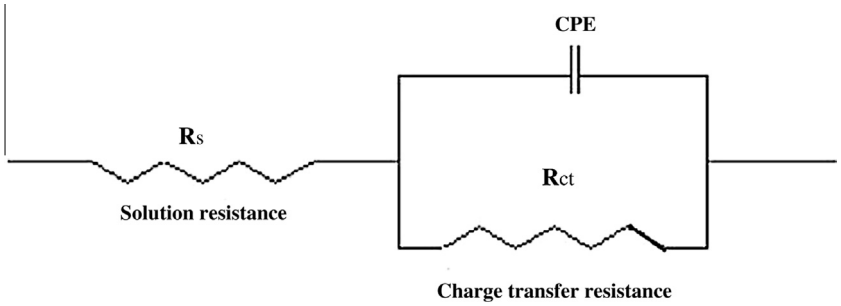

Figure 7 The suggested equivalent circuit model for the studied system.

Table 4 EIS parameters for corrosion of carbon steel in 1 M HCl in the absence and presence of different concentrations of the synthesized cationic surfactants at 25 °C.

Inhibitor	Conc. of inhibitor (M)	R_s Ω cm^2	Q_{dl} Ω^{-1} s^n cm^{-2}	n	Error of n	R_{ct} Ω cm^2	C_{dl} μF cm^{-2}	η_z %
1 M HCl	0.0	1.293	0.0002022	0.88	0.81	32.3	98.53	–
I	5.0×10^{-4}	4.206	0.0001807	0.74	1.09	86.68	164.4	62.74
	1.0×10^{-3}	3.502	0.0007489	0.66	1.60	147	76.65	78.03
	2.5×10^{-3}	5.496	0.0003231	0.68	1.14	198.9	56.95	83.76
	5.0×10^{-3}	1.752	0.0001959	0.721	1.05	210.7	26.88	84.67
	7.5×10^{-3}	4.772	0.000111	0.70	1.25	255.9	221.3	87.38
	1.0×10^{-2}	6.714	0.0006555	0.67	1.30	265.4	1.894	87.83
II	5.0×10^{-4}	8.563	0.0002199	0.78	0.70	94.64	75.33	65.87
	1.0×10^{-3}	8.911	0.001001	0.75	0.73	152.6	521.3	78.83
	2.5×10^{-3}	1.752	0.000111	0.70	1.25	210.7	26.88	84.67
	5.0×10^{-3}	4.957	0.000133	0.70	0.79	377.9	33.68	91.45
	7.5×10^{-3}	12.41	0.000334	0.72	0.96	401	141.2	91.95
	1.0×10^{-2}	7.608	0.000162	0.78	0.60	588.3	75.28	94.51
III	5.0×10^{-4}	8.911	0.001	0.75	0.74	152.6	521.3	78.83
	1.0×10^{-3}	4.772	0.0006555	0.67	1.30	255.9	221.3	87.38
	2.5×10^{-3}	7.958	0.0003269	0.62	0.99	346.6	72.53	90.68
	5.0×10^{-3}	4.827	0.0001644	0.62	0.89	434	29.33	92.56
	7.5×10^{-3}	1.509	0.0002376	0.71	0.74	514	110	93.72
	1.0×10^{-2}	6.303	0.0000594	0.71	0.84	608.3	16.53	94.69

inhibitors increases their η_I values. The maximum η_I values were obtained at 94.69 % for inhibitor III which insure that the tested inhibitors exhibit good inhibitive performance for carbon steel in 1 M HCl solution at 25 °C.

3.5. Adsorption isotherm and standard adsorption free energy

Basic information on the adsorption of inhibitor on metal surface can be provided by adsorption isotherm. Several isotherms including Frumkin, Langmuir, Temkin, Freundlich, Bockris–Swinkels and Flory–Huggins isotherms are employed to fit the experimental data. It is found that the adsorption of studied thiol cationic surfactants on carbon steel surface obeys the Langmuir adsorption isotherm equation [18]:

$$\frac{C}{\theta} = \frac{1}{K_{ads}} + C \tag{7}$$

where, C is the concentration of inhibitor, K_{ads} is the adsorptive equilibrium constant.

The degree of surface coverage values for various concentrations of thiol cationic surfactants in 1 M HCl solution has been calculated from the average of inhibition efficiency of potentiodynamic polarization Table 3. Plots of C/θ against C yield straight lines are shown in Fig. 8. Both linear correlation coefficient (r^2) and slope are close to 1, indicating the adsorption of the investigated inhibitors on the carbon steel surface obeys Langmuir adsorption isotherm. The adsorptive equilibrium constant (K_{ads}) can be calculated from the reciprocal of the intercept of C/θ–C curve. The values of K_{ads} were calculated from 5×10^{-4} M^{-1} for III. The high value of K_{ads} attributes to the stronger and more stable adsorbed layer formed on the metal surface. The standard free energy of adsorption (ΔG^o_{ads}) can be given as the following equation [19]:

$$\Delta G^o_{ads} = RT \ln (55.5 K_{ads}) \tag{8}$$

where, R is the gas constant (8.314 J mol^{-1} K^{-1}), T is the absolute temperature (K), and the value 55.5 is the concentration of water in solution expressed in molar.

The high values of K_{ads} and negative values of ΔG^o_{ads} suggested that, inhibitors molecules were strongly adsorbed on the carbon steel surface.

Values of ΔG^o_{ads} around −20 kJ mol^{-1} or lower are consistent with the electrostatic interaction between charged inhibitor molecules and the charged metal surface (physisorption); those around −40 kJ mol^{-1} or higher involve charge sharing or transfer from the inhibitor molecules to the metal surface

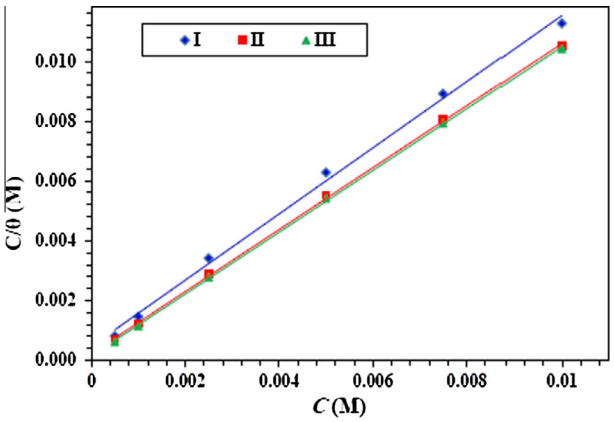

Figure 8 Langmuir's adsorption plots for carbon steel in 1 M HCl containing different concentrations of I, II and III at 25 °C.

to form a coordinate type of bond (chemisorption). The obtained values of ΔG^{o}_{ads}, for compounds I, II and III indicate that the adsorption takes place mainly through the electrostatic interaction between charged inhibitor molecules and the charged metal surface (physisorption and chemisorptions) [20]. The negative value of ΔH^{o}_{ads} indicates that the adsorption of investigated inhibitor on the carbon steel surface is exothermic. Entropy of inhibitor adsorption (ΔS^{o}_{ads}) is calculated using the following equation:

$$\Delta G^{o}_{ads} = \Delta H^{o}_{ads} - T\Delta S^{o}_{ads}. \quad (9)$$

Values of ΔS^{o}_{ads} are listed in Table 5. It is observed that, ΔS^{o}_{ads} values in the presence of the inhibitor have positive sign, which means that, an increase of disorder is due to the adsorption of only one surfactant molecule by desorption of more water molecules.

3.6. Inhibition mechanism

The adsorption of thiol cationic surfactants on the carbon steel surface in 1 M HCl solution occurs through the active centers in the inhibitors molecule which contain electronegative of SH, lone pair of N in pyridine ring and π-electrons of aromatic ring which they can easily adsorb on the metal surface and then reduce the anodic dissolution of carbon steel. It appears that inhibition occurred by a blocking mechanism on cathodic and anodic area of the metal surface (that is, inhibit both anodic and cathodic reactions) [21,22]. Polarization results showed that the inhibition effect of the inhibitors in 1 M HCl solution can be explained through that the nitrogen and sulfur atoms in the acid solution are protonated and regards as cationic species in addition cationic head of surfactant, which may be adsorbed on the cathodic sites of carbon steel surface and reduce the evaluation of hydrogen evaluation through the physical adsorption. While, counter ion (Br^{-}) may be adsorbed on the anodic sites of carbon steel surface and reduce the dissolution of metal through the physical adsorption. There is also another way of adsorption; the molecules can be adsorbed on the surface of carbon steel through the chemisorption mechanism that occurred by the donor–acceptor interactions between lone pair electron of hetero atoms and p-electrons of the pyridine ring of cationic surfactant and vacant d-orbitals of Fe atoms.

3.7. Surface active properties

3.7.1. Surface tension (γ)

Plot of γ versus concentration for 1-octyl, decyl, and dodecyl-4-mercapto pyridine-1-ium bromide is shown in Fig. 9. This figure shows two characteristic regions. At lower concentrations, the variation of surface tension is very significant, whereas at higher concentrations, it is relatively weak. The intercept of these two regions indicates the C_{cmc}. There are two antagonistic effects controlling the micellization, the hydrophobic group (alkyl chain) which is an important driving force in micellization and the hydrophilic group which opposes micellization. In our investigation, since the hydrophilic group is constant, we observe the C_{cmc} values of the prepared compounds decrease as the length of the alkyl chain increases as shown in Fig. 9. The surface tension values at the respective C_{cmc} (γ_{cmc}) values are given in Table 6. The results reveal that: the increase in hydrophobic chain length (III > II > I) makes the surfactant molecule more active at air/water interface.

The γ-log C plots also provide information about area per molecule, effectiveness and surface concentration of surfactant ions of the synthesized surfactant at air/water interface.

3.7.2. Effectiveness (π_{cmc})

Surface pressure at C_{cmc} which is defined as the effectiveness of a surfactant in reducing surface tension [23], is calculated from the following equation:

$$\pi_{cmc} = \gamma_{o} - \gamma_{cmc} \quad (10)$$

Table 5 The thermodynamic parameters of adsorption of the synthesized inhibitors at different concentrations for carbon steel in 1 M HCl solution.

Inhibitor	Temp. °C	K_{ads} M^{-1}	ΔG^{o}_{ads} kJ mol^{-1}	ΔH^{o}_{ads} kJ mol^{-1}	ΔS^{o}_{ads} J mol^{-1} K^{-1}
I	25	2745.0	−29.57	−9.87	66.10
	40	2123.1	−30.39		65.55
	60	1799.2	−31.87		66.07
II	25	4353.5	−30.71	−18.39	41.34
	40	2237.6	−30.52		38.77
	60	1960.4	−32.11		41.20
III	25	5000.0	−31.05	−19.40	39.12
	40	2310.5	−30.61		35.82
	60	2146.8	−32.36		38.93

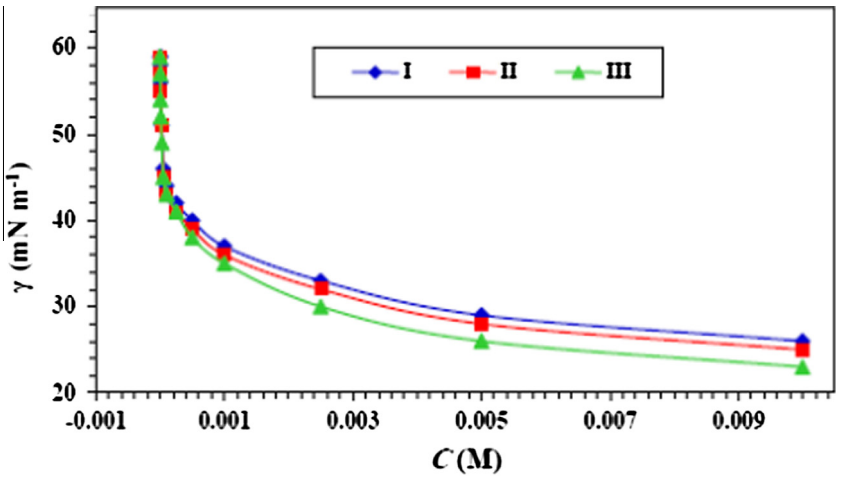

Figure 9 Variation of the surface tension with the synthesized cationic surfactants concentrations in water at 25 °C.

Table 6 Surface parameters of the synthesized cationic surfactants from both surface tension and conductivity measurements at 25 °C.

Inhibitor name	Surface tension measurements					Conductivity measurements		
	C_{cmc} M	γ_{cmc} mN m^{-1}	π_{cmc} mN m^{-1}	$\Gamma_{max} \times 10^{-11}$ mol cm^{-2}	A_{min} nm^2	C_{cmc} M	β	ΔG^{o}_{mic} kJ mol^{-1}
I	0.0028	30.2	41.8	7.6	2.20	0.0028	0.200	−26.61
II	0.0025	28.8	43.2	7.6	2.19	0.0026	0.157	−27.73
III	0.0023	26.1	45.9	7.7	2.17	0.0024	0.130	−28.45

where γ_o is the surface tension measured for pure water at the appropriate temperature and γ_{cmc} is the surface tension at critical micelle concentration. C_{cmc} value of the synthesized surfactant is listed in Table 6. The data showed that the surfactants are considered as a strong surface active agent at air/water interface. The results in Table 6 indicate that the effectiveness increases with the increase of the alkyl chain length in hydrophobic moiety of the synthesized surfactants which shows the effect of alkyl chain on the adsorption behavior of surfactant at air/water interface.

3.7.3. The surface excess (Γ_{max})

The maximum surface excess of the surfactant solution showed the number of surfactant molecules located in unit area at the air/water interface. Values of (Γ_{max}) represented in Table 6 show that increasing the hydrophobic character of the prepared compounds causes a corresponding increase in the Γ_{max} value. This indicates that the molecules are more tightly packed in the air/water interface in longer alkyl chain surfactants.

Maximum surface excess of a surfactant Γ_{max} at the air/solution interface is calculated from the maximal slope (d γ/d ln C) in the γ vs. ln C plot. In the absence of electrolyte, it is calculated by Gibbs adsorption equation [24]:

$$\Gamma_{max} = \frac{-1}{nRT} \times \frac{d\gamma}{d\ln C} \quad (11)$$

where C is denotes concentration, R is the gas constant, T is absolute temperature and n represents the number of species at the interface.

3.7.4. The area per molecule (A_{min})

The area per molecule, A_{min} (nm^2), at the interface provides information on the degree of packing and the orientation of the adsorbed surfactant molecule.

Increasing Γ_{max} indicates a larger number of adsorbed molecules at the air/water interface. Hence, the area available for each molecule at the interface will decrease. It is obvious from the data of A_{min} in Table 6 that increasing the alkyl chain length decreases the area occupied by each molecule.

The minimal surface area per adsorbed molecule, A_{min} (nm^2), is obtained as follows [25]:

$$A_{min} = \frac{10^{14}}{N_A \Gamma_{max}} \quad (12)$$

where N_A is the Avogadro number and Γ_{max} is the maximal surface excess of adsorbed surfactant molecules at the interface.

3.7.5. Conductivity measurements

Specific conductivity (K) measurements are performed for the synthesized cationic surfactant at 25 °C in order to evaluate the C_{cmc} and the degree of counter ion dissociation, β. It is well known that the specific conductivity is linearly correlated to the surfactant concentration in both the premicellar and in the postmicellar regions, and the slope in the premicellar region is greater than that in the postmicellar region [26]. The intersection point between the two straight lines gives the C_{cmc} while the ratio between the slopes of the postmicellar region to that in the premicellar region gives counter ion

dissociation; β. Fig. 10 shows the relation between specific conductivity and concentration of the synthesized surfactant. The values of degree of counter ion dissociation are calculated and listed in Table 6.

3.7.6. The standard free energy of micelle formation (ΔG^{o}_{mic})

Adsorption and micellization processes of the surfactant molecules are considered as phase transformation either from singly state molecule in the solution into adsorbed molecules at the interface (adsorption) or into the well aggregated molecules in the form of micelles (micellization).

The standard free energy of micelle formation per mole of surfactant is given by the equation [27]:

$$\Delta G^{o}_{mic} = (2-\beta)RT\ln C_{cmc} \quad (13)$$

where R is the gas constant, T is the temperature, β is the degree of counter ion dissociation and C_{cmc} is the concentration at critical micelle concentration, expressed in the molarity of the surfactant.

The value of ΔG^{o}_{mic} is calculated and listed in Table 6. From Table 6, the values of ΔG^{o}_{mic} and ΔG^{o}_{ads} are always negative indicating that these two processes are spontaneous; however, there is a slight increase in the negative values of ΔG^{o}_{ads} compared to those of micellization. This suggests a tendency of the molecules to be adsorbed at the interface rather than micellization in the bulk of the solution.

3.8. The relation between corrosion inhibition and surface properties of the prepared cationic surfactants

The highest reduction in surface tension (effectiveness, π_{cmc}) was achieved with increasing carbon chain length of cationic surfactants. This is in good agreement with the inhibition efficiency results which were achieved by cationic surfactants. It seems that the synthesized surfactants favor adsorption rather than micellization. The fact that ΔG^{o}_{ads} values were more negative compared with the corresponding ΔG^{o}_{ads} could be taken as strong evidence on the feasibility of the adsorption for the synthesized surfactants. It was noticed that the A_{min} values were increased, whereas the Γ_{max} values were decreased with increasing both the carbon chain length and corrosion inhibition efficiency of cationic surfactants. It was clear that inhibition efficiency increases with increasing Γ_{max} values and effectiveness and decreases with decreasing A_{min} values.

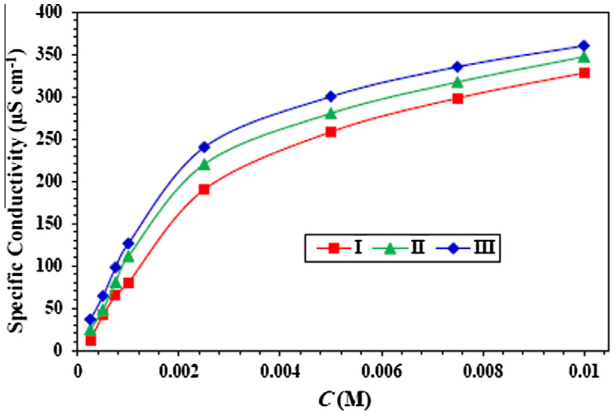

Figure 10 The plots of electrical conductivity against concentration of the synthesized cationic surfactants concentrations in water at 25 °C.

4. Conclusions

1. A new series of thiol cationic surfactants were synthesized and the chemical structure of these surfactants was confirmed by FTIR, ^{1}H NMR.
2. The inhibition efficiency of the synthesized cationic surfactant increased with an increase in its concentration and the alkyl chain length but it slightly decreases with an increase in temperature range 25–60 °C.
3. Double-layer capacitances decrease with respect to blank solution when the synthesized inhibitor is added. This fact can be explained by adsorption of the synthesized inhibitor species on the steel surface.
4. Tafel polarization curves indicate that the corrosion current density decreases very much and the corrosion potential changes little with the addition of the surfactant, therefore the synthesized inhibitor is a mixed type.
5. The adsorption of the synthesized cationic surfactant on the carbon steel surface represented a mixture of chemical and physical adsorption, it also obeyed Langmuir isotherm.
6. The inhibiting efficiencies obtained by polarization, EIS and weight loss measurements are in good agreement.

References

[1] B. Zerga, R. Saddik, B. Hammouti, M. Taleb, M. Sfaira, M. Ebn Touhami, S.S. Al-Deyab, N. Benchat, Int. J. Electrochem. Sci. 7 (2012) 631–664.
[2] O. Olivares, N.V. Likhanova, B. Gomez, J. Navarrete, M.E. Llanos-Serrano, E. Arce, J.M. Hallen, Appl. Surf. Sci. 252 (2006) 2894–2909.
[3] G. Bereket, E. Hur, C. Ogretir, J. Mol. Struct. (Theochem) 578 (2002) 79–88.
[4] S.K.A. Ali, M.T. Saeed, S.U. Rahman, Corros. Sci. 45 (2003) 253–266.
[5] M. Kissi, M. Bouklah, B. Hammouti, M. Benkaddour, Appl. Surf. Sci. 252 (2006) 4190–4197.
[6] A. Popova, E. Sokolova, S. Raicheva, M. Christov, Corros. Sci. 45 (2003) 33–58.
[7] M. Lagrenee, B. Mernari, M. Bouanis, M. Traisnel, F. Bentiss, Corros. Sci. 44 (2002) 573–588.
[8] E.S.H. El Ashry, A. El Nemr, S.A. Esawy, S. Ragab, Electrochim. Acta 51 (2006) 3957–3968.
[9] M.A. Quraishi, I. Ahamad, A.K. Singh, S.K. Shukla, B. Lal, V. Singh, Mater. Chem. Phys. 112 (2008) 1035–1039.
[10] I. Langmuir, J. Amer, Chem. Soc. 39 (1947) 847–848.
[11] N.A. Nabel, G.K. Nadia, A.B. Emad, A.M. Mohammed, Corros. Sci. 65 (2012) 94–103.
[12] S.A. Abd El-Maksoud, A.S. Fouda, Mater. Chem. Phys. 93 (2005) 84–90.
[13] A.M. Fekry, R.R. Mohamed, Electrochim. Acta 55 (2010) 1933–1939.
[14] S.E. Nataraja, T.V. Venkatesha, K. Manjunatha, B. Poojary, M. K. Pavithra, H.C. Tandon, Corros. Sci. 53 (2011) 2651–2659.
[15] G. Quartarone, L. Ronchin, A. Vavasori, C. Tortato, L. Bonaldo, Corros. Sci. 64 (2012) 82–89.
[16] S. Ramazan, A. Ece, K. Gülfeza, Mater. Chem. Phys. 125 (2011) 796–801.

[17] K. Hulya, K. Mustafa, D. Ilyas, S. Osman, Colloids Surf. A 320 (2008) 138–145.
[18] S. Ramazan, Corros. Sci. 52 (2010) 3321–3330.
[19] A. Ishtiaque, P. Rajendra, M.A. Quraishi, Corros. Sci. 52 (2010) 933–942.
[20] X. Li, D. Shuduan, F. Hui, Corros. Sci. 53 (2011) 302–309.
[21] E.M.S. Azzam, A.A. Abd El-Aal, Egypt. J. Pet. 22 (2013) 293–303.
[22] S.K. Shukla, M.A. Quraishi, Corros. Sci. 51 (2009) 1990–1997.
[23] S.A. Umoren, I.B. Obot, L.E. Apkabio, S.E. Etuk, Pigm. Resin Technol. 37 (2008) 98–105.
[24] S. Austin, C. Radhouane, D. Gaelle, C. Clarence, C.H. Patrice, J. Colloid Interface Sci. 320 (2008) 315–320.
[25] C. Gamboa, A.F. Olea, C. Gamboa, Colloids Surf. A 278 (2006) 241–245.
[26] M. Jitendra, V. Dharmesh, B. Prashant, Thermochim. Acta 428 (2005) 147–155.
[27] M.J. Rosen, Surface and Interfacial Phenomena, second ed., John Wiley & Sons, New York, 1989.